Materials Research, Vol. 6, No. 2, 219-226, 2003.

Correlation Between Fracture Toughness, Work of Fracture and Fractal Dimensions of Alumina-Mullite-Zirconia Composites

*Sérgio Francisco dos Santos, José de Anchieta Rodrigues**

Department of Materials Engineering, UFSCar
Federal University of São Carlos, 13565-905, São Carlos - SP, Brazil

Received: June 20, 2001; Revised: January 23, 2003

The purpose of this work is to show the correlation between the fractal dimension, D, and mechanical properties such as work of fracture, γ_{wof}, and fracture toughness, K_{Ic}. Alumina-mullite-zirconia composites were characterized by the slit-island method, SIM, to obtain values of D and its fractional part, D*. The fracture surface roughness was also evaluated using a cyclic voltametric method. It will be shown that there is a positive experimental dependency of γ_{wof} on D* and that there is not an evident correlation between K_{Ic} and D*.

Keywords: *work of fracture, fracture toughness, fractal dimension, roughness*

1. Introduction

Ceramic materials are extensively used for specific applications owing to their refractoriness and chemical stability. The brittleness of these materials, however, limits their applicability. Innumerable studies have focused on alternatives to offset this deficiency, and the development of microstructures with toughening mechanisms offers a possible solution[1].

To understand the action of the toughening mechanisms and to increase their effectiveness, it is necessary to study their action in the fracture process. This can be done by characterizing the fracture toughness, K_{Ic}, and the work of fracture, γ_{wof}, since these properties are related, respectively, to resistance to the onset of crack propagation and to total crack propagation process[2].

Another important area that contributes to the study of the fracture process of ceramic materials is quantitative fractography, a method by which one can analyze the "history" of the interaction between crack and microstructure and characterize the crack's surface roughness[3-8].

Surface roughness can be understood as geometrical irregularities on a smooth reference surface. The classic definition of roughness, R_s, is given by the ratio of the real surface area, A_R, to the projected area, A_0, (smooth reference surface)[3], which can be expressed as:

$$R_s = \frac{A_R}{A_0} \tag{1}$$

To avoid problems with the above definition of roughness it must be in mind that the smooth reference surface must be parallel to the average real fracture surface. In this work only this simple definition of roughness will be used because it describes exactly what is made experimentally to determine R_s.

Although the physical meaning of R_s is simple, it is not ease to obtain it directly by experimental means since it is very difficult to measure A_R. Therefore, R_s is usually evaluated indirectly through microscopic or nanoscopic techniques, or even using software for three-dimensional image analyses[7]. In addition, fractography involves several complex techniques, so roughness can be defined in a variety of ways and can, for instance, be measured by several topographic parameters, including real surface area[3-4], real length of a fracture profile[3-4], angular distribution[5-6], and the Fourier spectrum[8].

Despite the availability of various fractographic techniques and devices to evaluate roughness, fracture surfaces have yet to be adequately described. For this reason, the possibility of describing surfaces applying fractal geometry

*e-mail: josear@power.ufscar.br

is currently under discussion. From this standpoint, fractal geometry is also an alternative tool to describe roughness, because the real area of fracture surfaces can be related with fractal characteristics such as the fractal dimension, D, and the fractional part of the fractal dimension, D*. The following theoretical relationship between R_s and D* has been proposed by Mandelbrot[9]:

$$R_s = \eta^{-D^*} \tag{2}$$

where η is a non-dimensional parameter that is less than 1 and is related to the size of the ruler used to measure the length (or area). The fractional part of the fractal dimension, D*, is defined as the fractal dimension, D, minus the value 2 of the Euclidian dimension of a smooth surface.

Based on Eq. 2, some studies have attempted to correlate the fractal characteristics of a fracture surface to its roughness, also taking into account the material's microstructure[3,4,7,9,10].

Several studies have also attempted to correlate mechanical properties with the fractal dimension[10-18]. It has already been shown that, in the case of ceramic materials, the values of some mechanical properties increase when the fractal dimension increases. However must be emphasized that this is a very controversial subject and as an example, Charkaluk[16] must be addressed, who presents experimental data showing positive, negative and no correlation between fracture toughness and fractal dimension. Nagahama[17] deduced theoretically that it is possible a positive or a negative correlation depending on some microstructural parameter.

In the specific case of fracture toughness, K_{Ic}, it must be considered that this mechanical property is usually related to catastrophic fracture tests, e.g., K_{Ic}-test. Such property can only be indirectly related to the topographic features of the fracture surface, since a significant portion of the elastic energy stored during testing is released in the form of heat, sound, and kinetic propagation energy. The K_{Ic} property is associated to the onset of crack propagation while D is related to the fracture surface as a whole. Hence, it is not yet clearly understood how K_{Ic} can be experimentally related to D, although several proposals have been made[10,14,16-18]. Some are based on the Griffith-Irwin concept, which establishes that the critical elastic energy release rate, G_{Ic}, can be expressed, under plane stress condition[19], as:

$$G_{Ic} = 2\gamma_{ef} = \frac{K_{Ic}^2}{E} \tag{3}$$

where γ_{ef} is the effective fracture energy and E is the Young's Modulus.

Most models suggest that, to calculate K_{Ic}, the real surface area must be considered. Thus, γ_{ef} is calculated by multiplying the sum of the thermodynamic energy of the surface, γ_0, and that of the microplasticity at the tip of the crack, γ_p, by a fractal factor, η^{2-D}. Hence, the expression can be written as:

$$\gamma_{ef} \approx (\gamma_0 + \gamma_P) \cdot \eta^{2-D} \tag{4}$$

The association of Eq. 3 with Eq. 4 produces the following relation between K_{Ic} and D:

$$\frac{K_{Ic}^2}{E} \approx 2(\gamma_0 + \gamma_p) \cdot \eta^{2-D} \tag{5}$$

In Eq. 5, the fractal factor includes geometrical contributions of the microstructure to the fracture process of a polycrystalline material. Some works in the literature show good qualitative agreement between some proposed models and the results obtained from several brittle materials, however there are also controversies[14,17].

This paper seeks to verify the proposal that D or D* may be more adequately related to a mechanical property that reflects the average energy consumed by the crack during its entire propagation. This mechanical property could be the total energy of fracture, γ_{wof}. This property is evaluated along the complete fracture process through quasi-static crack propagation. Therefore, it can have a positive relation with the fractal dimension, which is also evaluated on the total fracture surface.

Rodrigues and Pandolfelli[12] proposed that, in ceramic materials in which only geometrical toughening mechanisms occur, a good correlation would be expected between the total energy of fracture, γ_{wof}, and D*. These geometrical toughening mechanisms cause the increase of total energy of fracture only through an increase of the real fracture surface area. Besides them, γ_{wof} is related with the total fracture process including the onset of the crack propagation. Another possible relation would be between the roughness, R_s, and the average resistance to crack propagation, $\langle R \rangle$. These relations can be expressed by[12]:

$$R_s = \frac{A_R}{A_0} = \frac{\gamma_{wof}}{\gamma_{ef}} = \frac{\langle R \rangle}{R_0} = \varepsilon_x^{2-D} = \varepsilon_x^{-D^*} \tag{6}$$

where R_0 is the first R-value of an R-curve and must be equal to 2 γ_{ef}. The average value of R, $\langle R \rangle$, is given by:

$$\langle R \rangle = \frac{1}{(\alpha_0 - \alpha_f)} \int_{\alpha_0}^{\alpha_f} R(\alpha) d\alpha \tag{7}$$

where α_0 and α_f represent relative notch size and relative final crack length, respectively, for a sample subjected to a stable crack propagation test in order to obtain the R-curve.

From the standpoint of the fractal theory, the parameter ε_x in Eq. 6 represents only the relative size of a length measure unit, as represented by η in Eq. 2. If this were real, then R_s could not have a specific value that characterizes a fracture surface. Hence, ε_x could represent a non-dimensional construction unit of the fracture surface, which would have to be less than 1, and would be measurable by some microscopy technique.

Si_3N_4-SiC composites were tested by Pezzotti and coworkers[13], who experimentally found a relation between γ_{wof} and a fractal parameter. However, these researchers proposed no parametric relation involving either D and γ_{wof} or D and $\langle R \rangle$, although they obtained the R-curves of those composites.

This paper, therefore, discusses the experimental relation between D* and the mechanical properties, K_{Ic} and γ_{wof}, for alumina-mullite-zirconia composites with different amounts of mullite and zirconia phases. Electrochemical cyclic voltametry was also employed to measure the roughness of the fracture surfaces.

2. Experimental Procedure

2.1 Materials

The alumina-mullite-zirconia composites used for this study were prepared and their physical and thermomechanical properties characterized by Mazzei *et al.*[20,21]. The samples were prepared by reaction sintering of alumina and zircon, using 0, 5, 10 and 15 wt% of zircon to produce the different composites. Samples with 62 mm × 6 mm × 5 mm dimensions were obtained through 60 MPa uniaxial pressing followed by sintering at 1650 °C for 2 h. The final phase compositions are shown in Table 1.

Figure 1 shows the typical microstructure of the composite prepared with 85 wt% of alumina and 15 wt% of zircon.

2.2 Mechanical characterization

An MTS model 810/458-series universal testing machine was used for the mechanical characterization. A 3-point bending test on machined samples was applied to obtain K_{Ic} and γ_{wof} values. Sets of at least 3 samples were employed in each test condition with the aim of obtain average values for the properties.

Load, P, *vs.* displacement, d, curves with catastrophic propagation were used to determine K_{Ic}. Mazzei *et al.*[20,21] applied the conditions of plane strain established by ASTM E399-81[22]. The four-faces machined samples for this test were straight notched applying a diamond-coated disk of 150 μm in thickness. The notch depth was 30% of the sample height to facilitate the catastrophic propagation of the crack. The final dimensions of the sample were approximately 55 mm × 5 mm × 4 mm, being the 5-mm dimension oriented to be the height of the sample. A span of 40 μm was used in the 3-point bending arrangement. An actuator velocity of 5 mm/min was applied on samples C1 to C3, while 7 mm/min was applied on sample C4.

P *vs.* d curves, obtained from stable crack propagation tests, were used to obtain γ_{wof}-values under 3-point bending condition. The actuator velocity used in this case was 1 μm/min. The samples for these tests were prepared with a 90° Chevron notch, applying a 400 μm in thickness diamond-coated disk. The tip of the Chevron notch was at 30% of the sample height. The final dimensions of the samples and the orientation of them in the bending test were the same already described for the fracture-toughness test. The final values of γ_{wof} were calculated using the value of the work required to reach complete fracture divided by double the projected fracture area.

Table 2 shows the values of K_{Ic} and γ_{wof} obtained by Mazzei *et al.*[20,21].

Table 1. Compositions produced for the alumina-mullite-zirconia composites used in this work[20,21].

Composite designation	Raw materials (weight-%)		Contents of Al_2O_3, ZrO_2 and mullite (weight-%)		
	Al_2O_3	$ZrSiO_4$	Al_2O_3	ZrO_2	Mullite
C1	100	0	100.0	0.0	0.0
C2	95	5	89.5	3.9	6.7
C3	90	10	79.1	7.7	13.3
C4	85	15	68.9	11.4	19.7

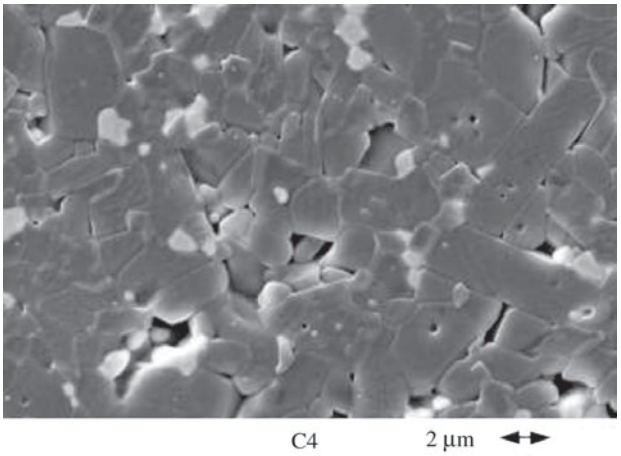

Figure 1. Example of the microstructure of the C4-composite obtained by SEM.

Table 2. Mechanical properties of the alumina-mullite-zirconia composites[20,21].

Composite designation	K_{Ic} (MPa.m$^{1/2}$)	γ_{wof}(J/m^2)
C1	5.3 ± 0.3	34 ± 4
C2	5.3 ± 0.1	50 ± 3
C3	5.4 ± 0.3	52 ± 3
C4	5.6 ± 0.03	67 ± 3

2.3 Characterization of the composites' fracture surfaces

The fractal dimension, D, was obtained applying the slit island method, SIM, proposed by Mandelbrot *et al.*[11], using the following steps[15]:

i. preparation of the fracture surface with a gold film deposited with a conventional Balzers sputtering device;

ii. castable cold mounting of the fractured sample so that the medium fracture plane lay parallel to the imaginary polishing plane;

iii. grinding and polishing were carried out with a semi-automatic Minimet/Buehler machine. 400 and 600 grade sandpaper was used to remove the excess resin from the surface, followed by 9, 6, 3, and 1 μm diamond paste to reveal the first island contours. From then on, only 1 μm diamond paste was used, alternating polishing (wear) and fractal measurements;

iv. perimeter and area measurements were taken of the islands using a Labophot-2/Nikon microscope with 100× magnification lens. A Synoptics Optamax V image analysis system was employed to facilitate the characterization. Considering the whole system used, the resulting ruler size (measurement unit) was 0.54 μm. At least 5 levels of wear were analyzed for each fracture surface. At least 4 to 8 different regions of the same surface were analyzed for each wear level. Besides this, both fracture surfaces of each sample were examined for a more representative measurement of fractal characteristics. At least 3 samples were used for each test condition.

Area-*vs.*-perimeter graphs were plotted on a logarithmic scale. By linear regression, the angular coefficients of the straight lines were obtained. The corresponding D-values were calculated using the following equation:

$$\log(\text{area}) = C + \left(\frac{2}{D}\right) \cdot \log(\text{perimeter}) \qquad (8)$$

where C is a constant[9-11].

The sharpness of the island boundaries in the image analysis equipment depends, among other factors, on the how the sample was prepared, how long it was polished, and its cleanliness, as well as lighting, magnification, and focal distance of the equipment. To minimize the influence of these factors on the evaluation of the fractal dimension, an experimental procedure was adopted based on suggestions given by Russ[23], i.e., only areas in the range of 400 μm^2 to 8000 μm^2 were measured with 100× magnification.

An adapted cyclic voltametric method[15] was applied to measure the average voltametric roughness, R_v, with the purpose of evaluating the differences in roughness from one composite to another and to verify the relation between roughness and the fractal factor, $\varepsilon_x^{-D^*}$, established by Eq. 6.

3. Results and Discussion

Figure 2 shows a typical optical image from slit islands of the alumina sample's fracture surface, composition 1, C1, after several wear/polish steps. The slit islands are highlighted in the photo by bright regions surrounded by dark boundaries, which are promoted by the deposited gold layer.

Four examples of log (area) *vs.* log (perimeter) graphs resulted from the application of SIM on alumina-mullite-zirconia composites are shown in Fig. 3. The increment of the fractal dimension values, D* = D - 1.00 were calculated based on these graphs. The value of 1.00 rather than 2.00 appears here because, for SIM, the island boundaries are fractal and their reference dimension is therefore equal to 1.00. This investigation was also based on the assumption

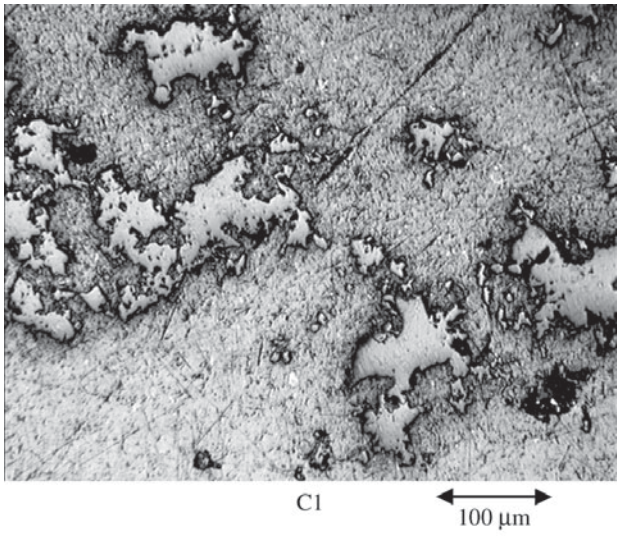

Figure 2. Example of the slit islands of the fracture surface of the C1-composition obtained by SIM. The bright regions with dark contours represent the islands.

that the fractal dimension of the fracture surface is equal to the fractal dimension of the slit island boundary plus 1 unit[9,11].

The graphs in Fig. 3 also show the straight lines obtained by linear regression, whose linearity can be verified by correlation factors equal or greater than 0.90. The D*-values were obtained from the angular coefficient of the straight line, using Eq. 8. Table 3 illustrates these D*-values, while Fig. 4 plots these values as a function of the zircon content in the reaction.

Although the errors in D* are a little bit big, Fig. 4 appears to indicate, a weak positive correlation between D* and the zircon content in the reaction, which in turn determines the zirconia and mullite content in the composites, as shown in Table 1. Therefore, it can be thought that incrementing the content of these phases in the form of dispersed particles leads to an increase of the fracture surface's fractal dimension. It is believed that zirconia and mullite particles generate the microcracking phenomenon[20,21], which in turn affects the fractal dimension. It should be kept in

Table 3. D* values of the fracture surface of alumina-mullite-zirconia composites obtained by SIM. The value of the ruler length was 0.54 μm.

Composite designation	Zircon content in the reaction (weight%)	D* (ad.)
C1	0	0.47 ± 0.09
C2	5	0.55 ± 0.08
C3	10	0.58 ± 0.04
C4	15	0.7 ± 0.1

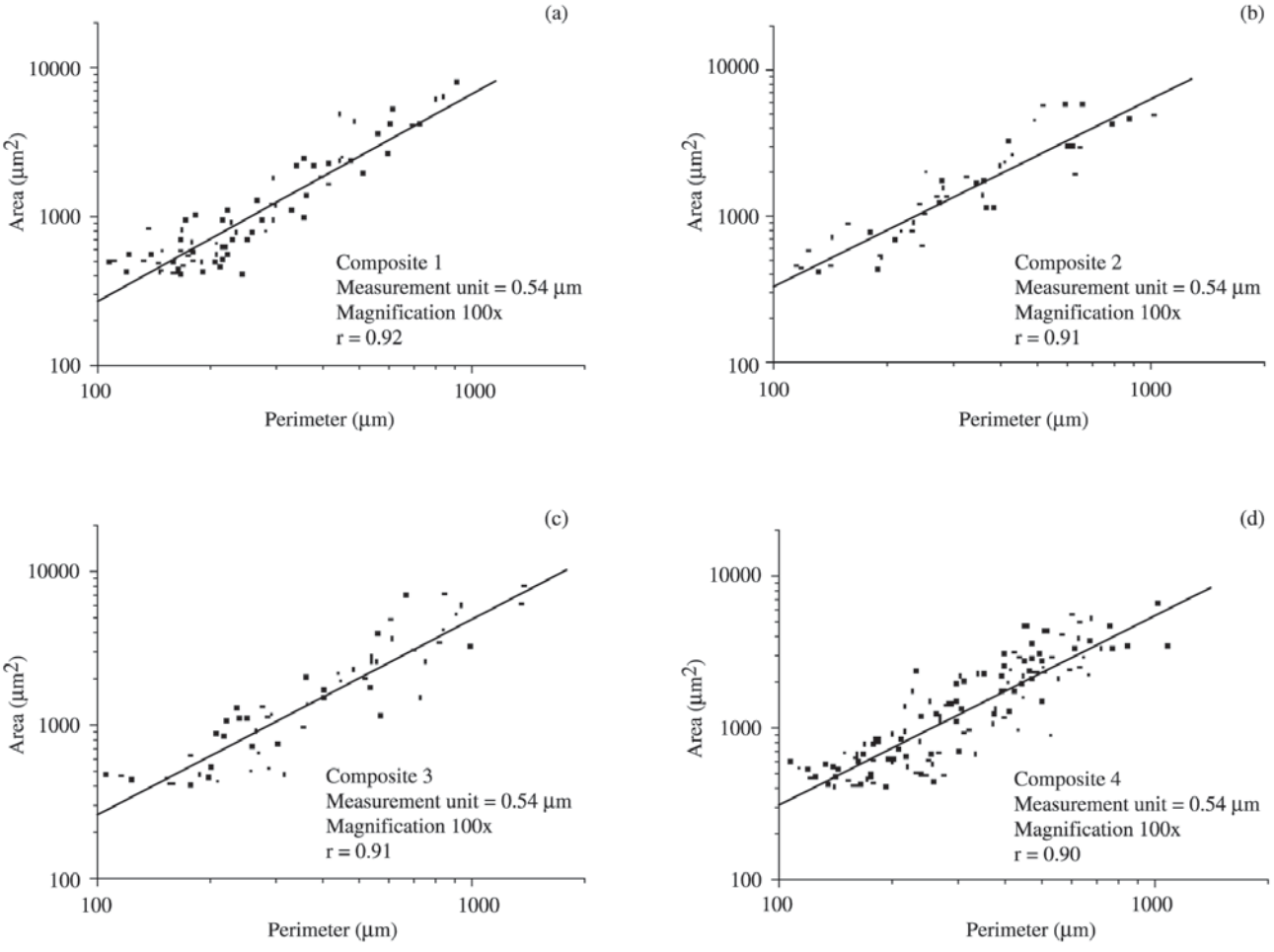

Figure 3. Examples of log(area) × log(perimeter) graphs of the alumina-mullite-zirconia composites that were used to obtain D*-values. (a), (b), (c), and (d) show plots for the C1, C2, C3, and C4 compositions of Table 1, respectively. The r-values shown in the captions of the graphs are the correlation factor of the linear regressions.

mind that the microcracking toughening mechanism is associated with other mechanisms of a geometrical nature, which can directly contribute to the building of the fracture surface's topography. Among other mechanisms, crack deflection and crack branching are very significant. Therefore, SIM was sufficiently sensitive to detect topographic differences in the fracture surfaces caused by changes in the composite's microstructure.

Table 4 presents the values of the average voltametric roughness, R_v, for the materials investigated in this work.

From Table 4 it can be inferred that R_v does not depend on the zircon content in the composites' formation reaction. On the other hand, considering experimental errors, the measured R_v-values agree with the estimated roughness R_s-values for alumina reported in the literature. Dörre and Hübner[24] state that the fracture surface of a typical polycrystalline alumina presents a real area that is 2 to 4 times larger than its projected area. However, we believe that the composites' fracture surfaces used in our investigation would show differing topographies, since the concentration of dispersed zirconia and mullite particles also varied. Furthermore, these composites presented increasing porosity with greater zircon content due to the dissociation occurring during the reaction of this raw material[20,21]. Hence, the possibility that the electrochemical method is insensitive to minor differences in fracture surface roughness cannot be discarded.

Table 4. R_v-values of the fracture surface of alumina-mullite-zirconia composites. The samples used for this characterization were the same as those used for the γ_{wof}-tests.

Composite designation	Zircon content in the reaction (weight-%)	R_v (ad.)
C1	0	4.0± 0.9
C2	5	4 ± 1
C3	10	3.9 ± 0.9
C4	15	3.9 ± 0.9

Tables 1 and 2 indicate a positive correlation between γ_{wof} and the zirconia and mullite content, but not an evident correlation between K_{Ic} and those particles content. It is presumed that this fact results from the sensibility of the γ_{wof}-test in recording the contribution of microcracking to the fracture process as a whole. This statement is corroborated by the fact that MEV-micrographs show microcracks associated to the nearby region of zirconia particles in alumina grains, as shown in Fig. 5 for the composite C4. Although not shown here, it was found that this microcracking did not occur in the pure alumina sample (composition C1 in Table 1)[20,21].

Figure 6 shows that there is not an evident correlation between K_{Ic} and D* for the alumina-mullite-zirconia composites studied in this work, since the correlation factor of the linear regression is so low as 0.71. The absence of correlation illustrated in Fig. 6 agrees, to a certain extent, with the uncertainties about the clear relation between K_{Ic} and D* reported in the literature for distinct material classes, including ceramics[16].

Plotting the log (γ_{wof}) *vs.* D*, however, the linear regression indicates a correlation factor of 0.96, as shown in Fig. 7. As discussed earlier herein, the increment in D*-values due to the increasing zircon content in the reaction is assumed to be associated to the microstructure's increased microcracking. However, one must also take into account that other toughening mechanisms may have acted upon

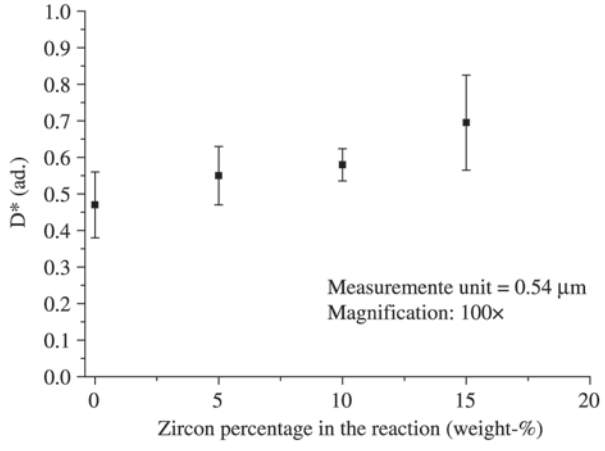

Figure 4. D* values *vs.* zircon concentration for the alumina-mullite-zirconia composites.

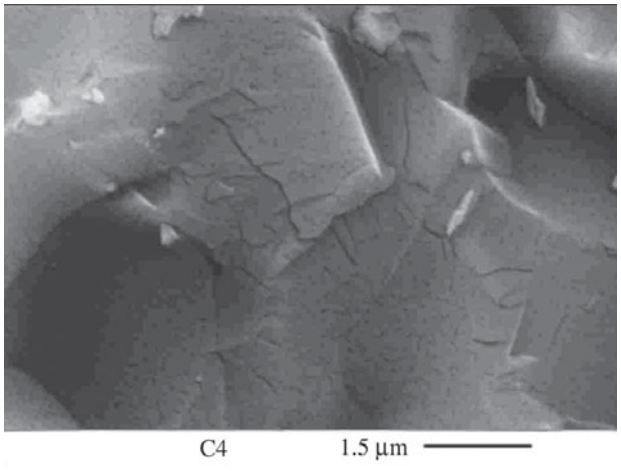

Figure 5. Details of a micrograph of the fracture surface of the C4-composition showing microcracking.

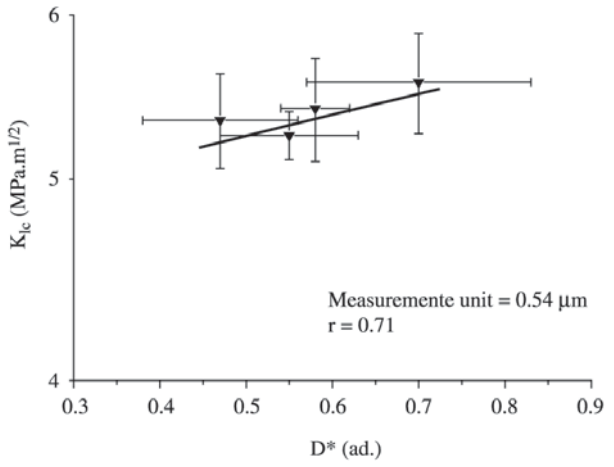

Figure 6. K_{Ic} versus D* monolog-graph for the alumina-mullite-zirconia composites. The r-values are the correlation factor of the linear regression.

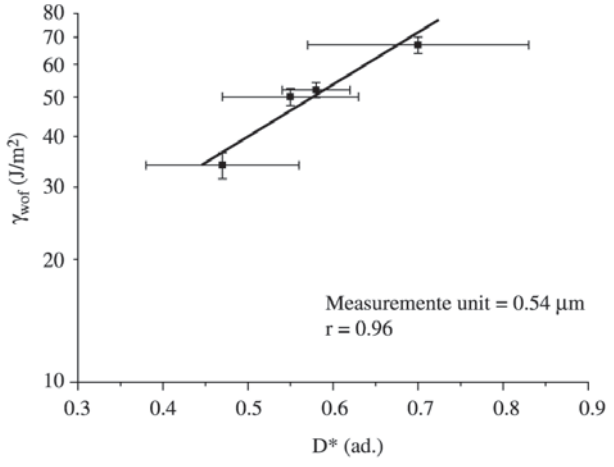

Figure 7. γ_{wof} *vs.* D*monolog-graph for the alumina-mullite-zirconia composites. The r-values are the correlation factor of the linear regression.

the composites studied here, involving a certain volume beneath the fracture surfaces and also consuming fracture energy. This, in turn, would have further contributed to the increase in γ_{wof} without necessarily disturbing the characteristics of the fracture surface.

Lastly, it can be said that these results are consistent, since the materials studied here presented mainly toughening mechanisms that acted geometrically and contributed to the topography of the fracture surface. It should be kept in mind that the zirconia generated "in situ" is neither partial nor totally stabilized. The zirconia was, therefore, of the monoclinic type and the resulting microcracks were caused by post-sintering cooling[20,21]. Thus, the change in γ_{wof}-values as a function of D* depends on the extent to which these mechanisms participate in the fracture process and how this reflects on the development of the fracture surfaces. Consequently, the statement of Rodrigues and Pandolfelli[12] about ceramic materials is correct, i.e., the total fracture energy is expected to rise with the increasing real area of the fracture surface when only purely geometric toughening mechanisms occur. The monologarithmic plot of γ_{wof} *vs.* D*, in Fig. 7, corroborates the proposed relation given in Eq. 6.

4. Conclusions

The average voltametric roughness, R_v, is apparently not dependent on zirconia and mullite phase concentrations in the case of fracture surfaces of the alumina-mullite-zirconia composites studied in this work.

However, R_v-values found in this work are realistic and agree with reported values of other researchers.

There is not an evident positive relation between fracture toughness, K_{Ic}, and the fractal dimension, D, when the zirconia and mullite phase concentration was increasingly changed in the alumina-mullite-zirconia composites of this study. In the technical literature it is possible to find reports about positive, negative, and no correlation between the two mentioned parameters.

It was also found that there is a positive correlation between γ_{wof} and D* in the alumina-mullite-zirconia composites studied in this work. This emphasizes the fact that D* is far more appropriately related to a mechanical property directly associated with the average energy consumed by the crack throughout its entire propagation.

Acknowledgements

The authors gratefully acknowledge the financial support of FAPESP (Process Nº 96/01988-2) for this work. Thanks are also due to MSc. Ângela C.A. Mazzei for the composite samples, and to Prof. Dr. Carlos Alberto Avaca, University of São Paulo and Dr. Carlúcio Roberto Alves, Ceará State University, for their technical cooperation in applying the cyclic voltametric method. Last but not least, the authors thank Alcoa Alumínio S/A for its donation of the raw materials used in this study.

References

1. Steinbrech, R.W. - Toughening mechanisms for ceramic materials**,** *J. Eur. Ceram. Soc*., v. 10, p.131-142, 1992.
2. Sakai, M.; Bradt, R.C. - Fracture toughness testing of brittle materials, *International Materials Reviews*, v. 38, n. 2, p. 53-78, 1993.

3. Banerji, K. - Quantitative Fractography: A Modern Perspective, *Metall. Transactions A*, v. 19, n. 4, p. 961-971, 1988.
4. Underwood, E.E.; Banerji, K. - Invited Review: Fractals in fractography, *Material Science and Engineering*, v.80, p. 1-14, 1986.
5. Gokhale, A.M.; Underwood, E.E. - A general method for estimation of fracture surface roughness: Part I. Theoretical Aspects. *Metall. Transactions A*, v. 21A, n. 5, p. 1193-1199, 1990.
6. Gokhale, A.M.; Drury, W.J. - A general method for estimation of fracture surface roughness: Part II. Practical Considerations. *Metall. Transactions A*, v. 21A, n. 5, p. 1201-1207, 1990.
7. Lange, D.A.; Jennings, H.M.; Shah, S.P. - Relationship between fracture surface roughness and fracture behavior of cement paste and mortar, *J. Am. Ceram. Soc*., v. 76, n. 3, p. 589-597, 1993.
8. Passoja, D.E.; Amborski, D.J. - Fracture profile analysis by Fourier transform methods, *Microstrut. Sci*., v. 6, p. 143-148, 1978.
9. Mandelbrot, B.B., *The fractal geometry of nature*, 3 ed., New York-USA, W.H. Freeman and Company, p. 468, 1983.
10. Xin, B.Y. et. al. - Quantitative characterization of the fracture surface of Si single crystals by confocal microscopy, *J. Am. Ceram. Soc*., v. 78, n. 12, p. 3201-3208, 1995.
11. Mandelbrot, B.B.; Passoja, D.E.; Paullay, A.J. - Fractal character of fracture surfaces of metals, *Nature,* v. 308, n. 4, p. 721-722, 1984.
12. Rodrigues J.A.; Pandolfelli, V.C. - Insights on the fractal-fracture behaviour relationship, *Materials Research*, v. 1, n. 1, p. 47-52, 1998.
13. Pezzotti, G *et. al.* - Fractal character of fracture surfaces and boundary values of toughness in simple ceramic-ceramic system, *Materials Science and Engineering A*, v. 197, p. 109-112, 1995.
14. Tanaka, M. - Fracture toughness and crack morphology in indentation fracture of brittle materials, *J. Mat. Sci*., v. 31, p. 749-755, 1996.
15. Santos, S.F. - *Application of the fractals concept for analysis of the fracture process in ceramic materials*, São Carlos, 1999, 193p. Master's Thesis, Programa de Pós-Graduação em Ciência e Engenharia de Materiais, Universidade Federal de São Carlos (in portuguese).
16. Charkaluk; E.; Bigerelle; M.; Iost, A. - Fractals and fracture, *Engineering Fracture Mechanics*, v. 61, p. 119-139, 1998.
17. Nagahama, H. - A fractal criterion for ductile and brittle fracture, *J. Appl. Phys.* v. 75, n. 6, p. 3220-3222, 1994.
18. Mecholsky, Jr. J. J.; Freiman, S.W. - Relationship between fractal geometry and fractography, *J. Am. Ceram. Soc.,* v. 74, n. 12, p. 3136-3138, 1991.
19. Broek, D. - *Elementary engineering fracture mechanics* - Martinus N. Publishers, Boston, p. 469, 1983.
20. Mazzei, A.C., Rodrigues, J.A. – Alumina-mullite-zirconia composites obtained by reaction sintering – Part I Microstructure and mechanical behaviour, *J. Mat. Sci.*, v. 35, p. 2807-2814, 2000.
21. Mazzei, A.C., Rodrigues, J.A., Pandolfelli, V.C. – Alumina-mullite-zirconia composites obtained by reaction sintering – Part II R-Curve behaviour, *J. Mat. Sci.*, v. 35, p. 2815-2824, 2000.
22. Standart Test Method for Plane Strain Fracture Tougheness of Metallic Materials, E399-81.
23. Russ, J.C. - *Fractal Surfaces*, Plenum Publishing Corp, 1st ed., New York-USA, p. 309, 1994.
24. Dörre, E., Hübner, H. - *Alumina processing, properties and applications*, 1st ed., Berlin - German Springer-Verlag, p. 329, 1984.